Supporting Information

Following the formation of silver nanoparticles using *in-situ* X-ray absorption spectroscopy

Ian J. Godfrey,[†,‡] *Andrew J. Dent,*[§] *Ivan P. Parkin,*[†] *Shinya Maenosono*[‡*] *and Gopinathan Sankar*[†*]

[†]Department of Chemistry, University College London, 20 Gordon Street, London, WC1H 0AJ, United Kingdom

[‡]School of Materials Science, Japan Advanced Institute of Science and Technology, 1-1 Asahidai, Nomi City, Ishikawa, 923-1292, Japan

[§]Diamond Light Source, Harwell Science and Innovation Campus, Didcot, Oxfordshire, OX11 0DE, United Kingdom

*GS: g.sankar@ucl.ac.uk SM: shinya@jaist.ac.jp

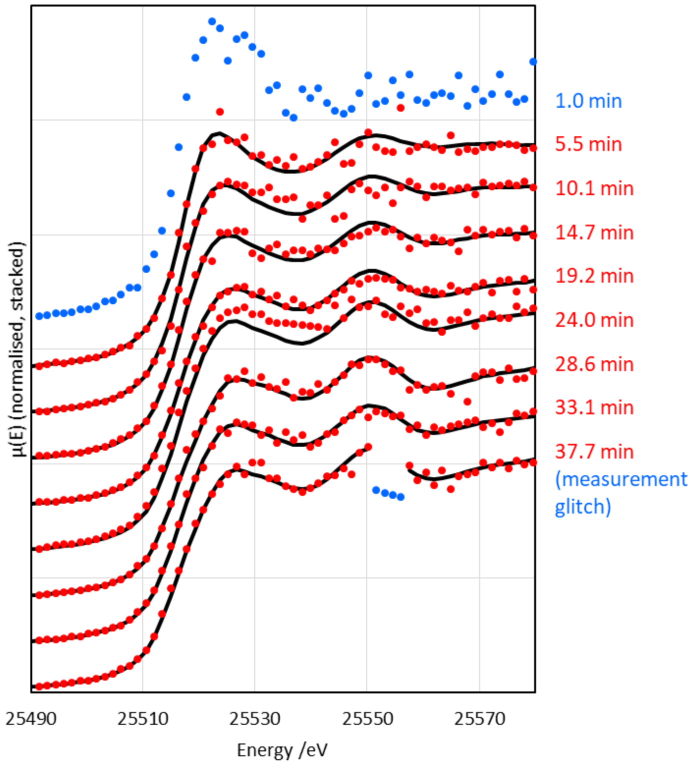

Figure S1: LCF fits (black lines) and unsmoothed Ag K-edge XANES data (red points) for all scans from Figure 1. Note – the fits are those from Figure 1 and were fitted to the smoothed data, they are displayed to confirm their consistency with the unsmoothed data. Also shown is the XANES at one minute (which was not used as the data quality was inadequate) and a four-point measurement glitch in the 37.7 minute XANES that was excluded from the fitting.

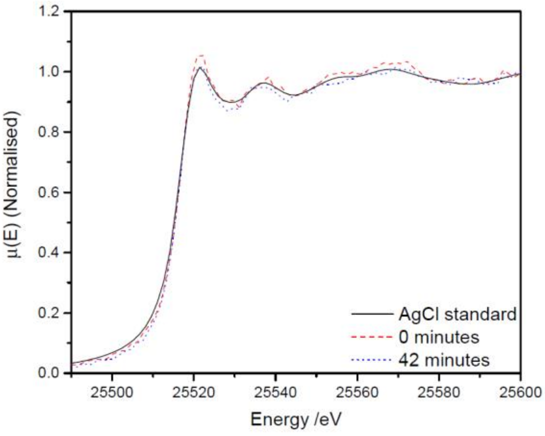

Figure S2: Stability of a mixture of $AgNO_3$ and $HAuCl_4$ in the beam (under reaction conditions, but without trisodium citrate) at the Ag K-edge

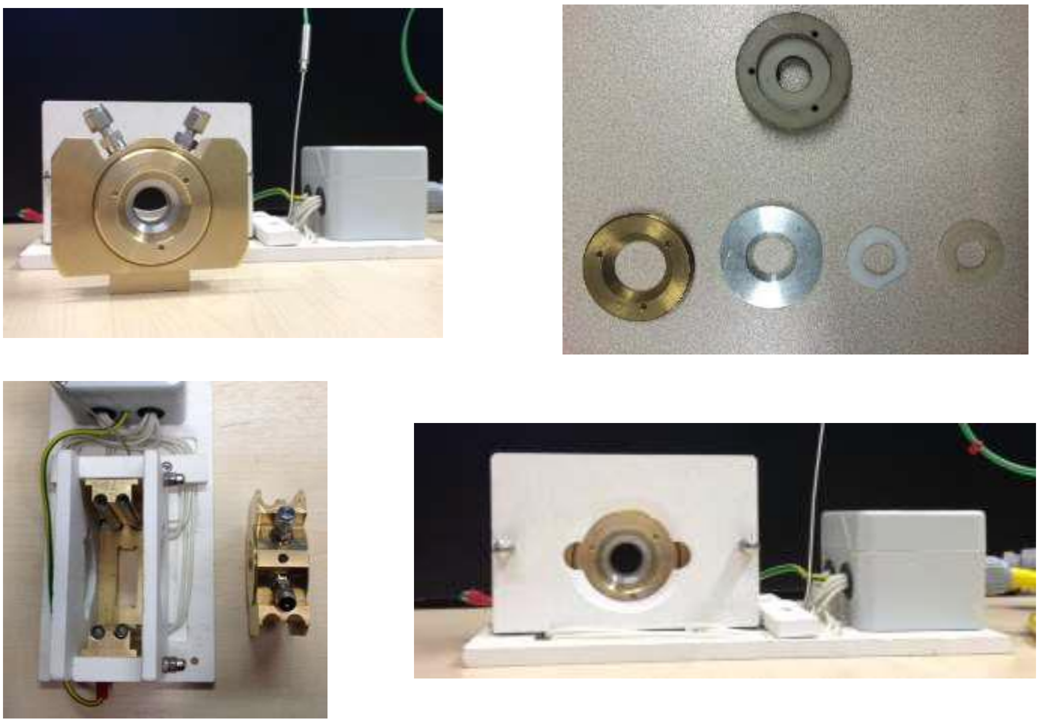

Figure S3, clockwise from top left: assembled *in-situ* cell and heated stage (the Swagelok connectors can be used as injection ports or connected to a gas or stop-flow system), cell components - polyetheretherketone spacer (with conduits drilled through for chemical injection) and (in order) mica/Kapton windows (not shown), silicon, Teflon, aluminium and brass rings used to seal the cell (the brass ring and the cell both have screw threads, allowing the cell to be sealed/opened simply by screwing the brass ring in/out), cell fully assembled in heated stage, top view of the cell and heated stage. Photographs reproduced from.[1] Photographs courtesy of A Mantalidi. Copyright 2016.

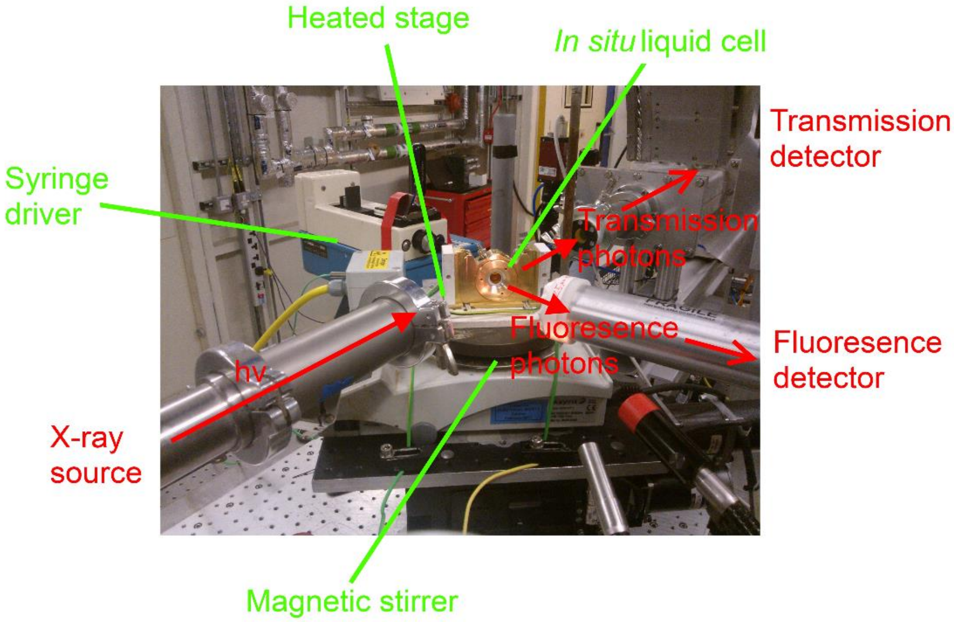

Figure S4: The *in-situ* cell set up on B18 for these experiments. Background photograph reproduced from[1]. Background photograph courtesy of A Mantalidi. Copyright 2016.

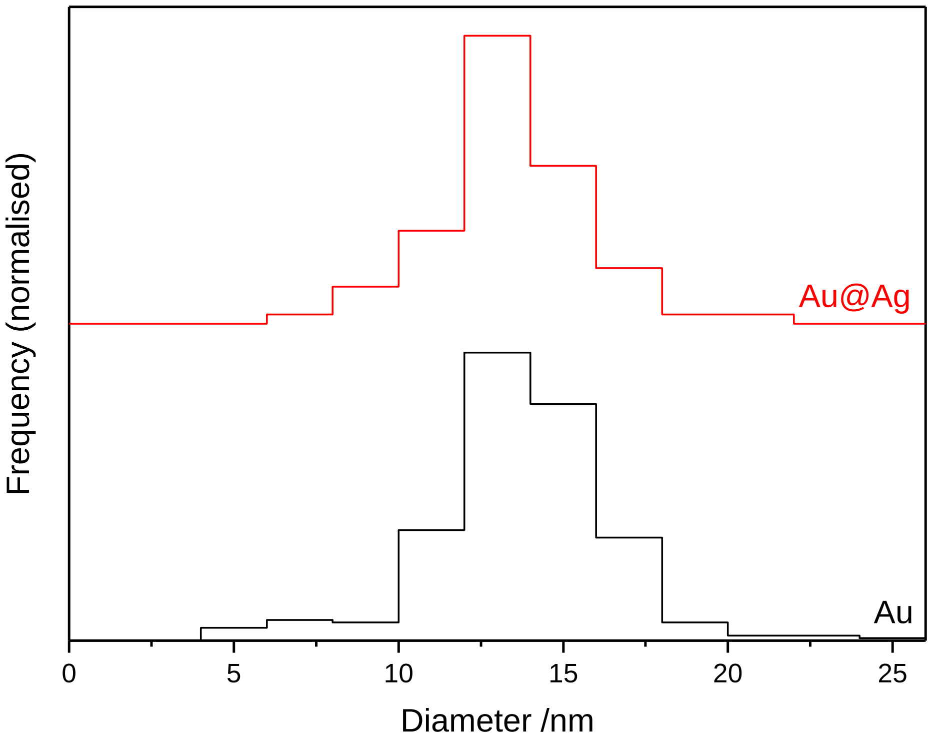

Figure S5: Size distributions of the gold seed particles and cores in the Au@Ag particles during a typical lab synthesis, showing that gold particles are not substantially affected by the reaction. Based on data previously published in [2].

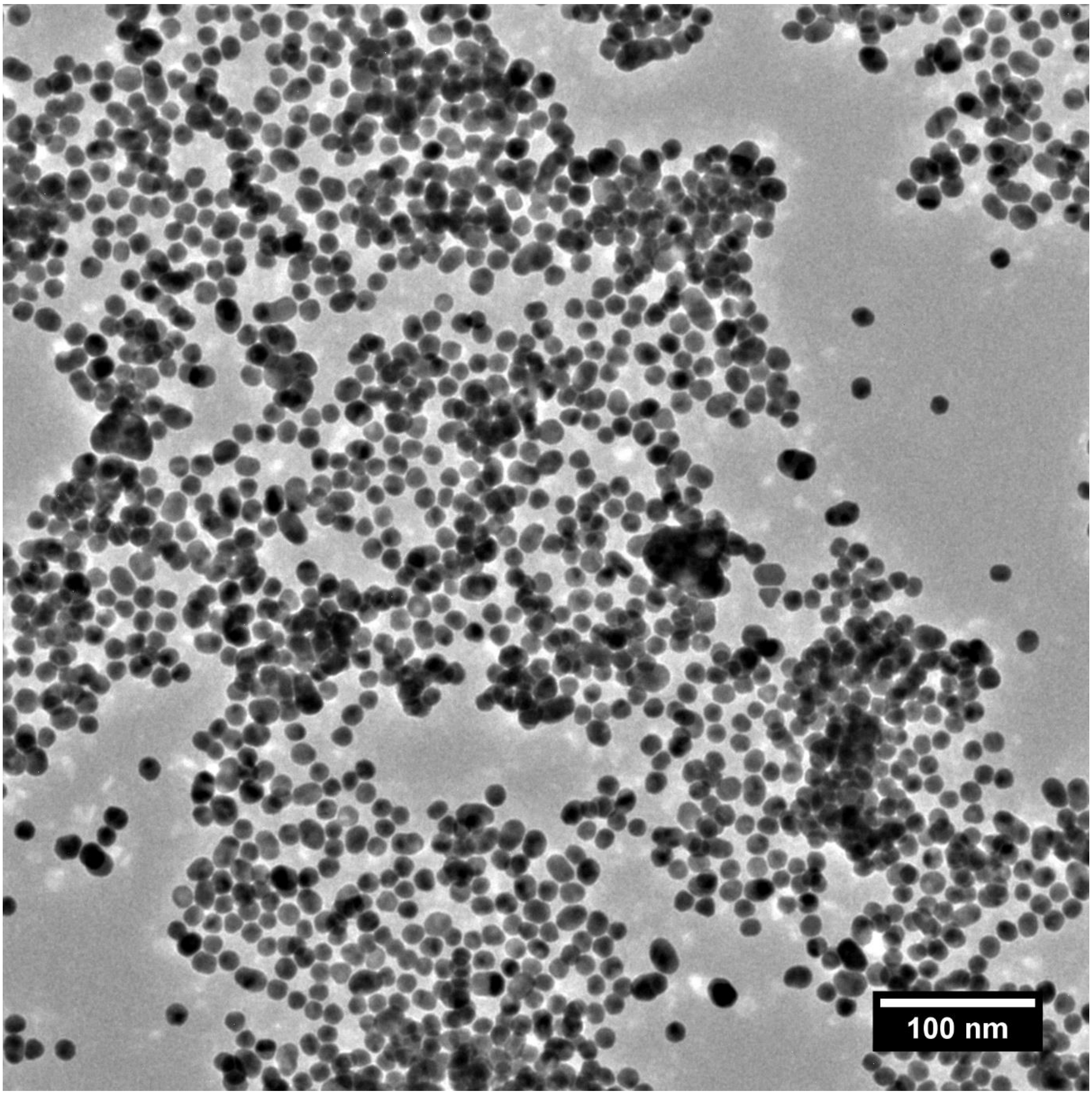

Figure S6: TEM image of the gold seed colloid used for the *in-situ* XAS studies.

To verify the crystalline nature of the nanoparticles, *ex-situ* high-resolution transmission electron microscopy (HRTEM) and X-ray diffraction (XRD) were performed on samples prepared according to a lab synthesis. The samples were prepared according to the synthesis detailed in[2].

Prior to recording the XRD patterns, the colloids were immobilised onto silica nanospheres by sonicating at pH 1-2 (pH adjusted with 0.1 M H_2SO_4); a weight loading of 1 % was targeted. The mixture was then centrifuged (6000 RPM, 2-3 min) and the slurries dried in air (128 °C, 8 h). This procedure was based on that reported by Luo *et al.*[3]

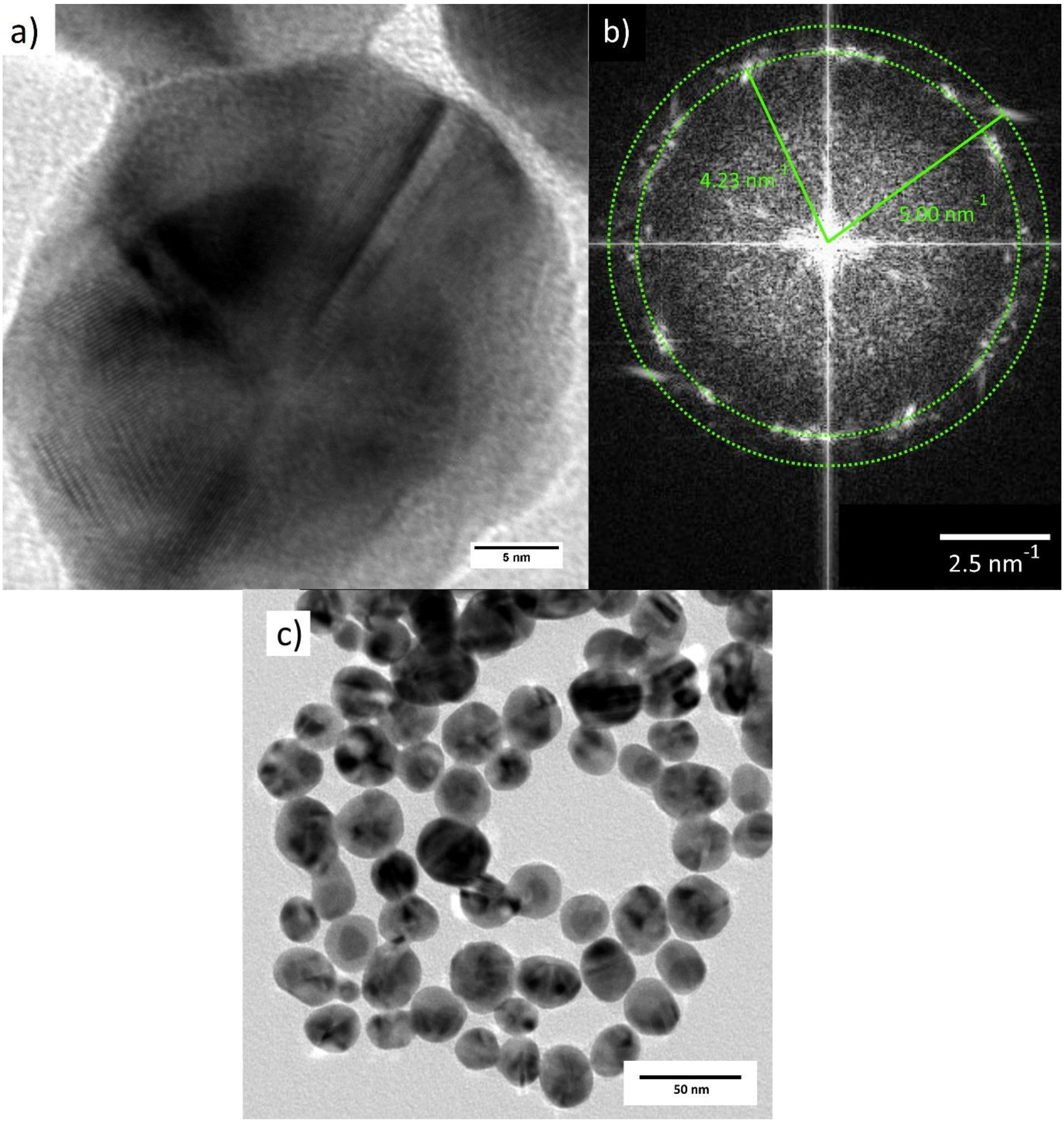

Figure S7: HRTEM (a) of an Au@Ag nanoparticle, and reduced fast Fourier transform of the HRTEM (b). The HRTEM clearly displays lattice fringes, these are visible in the FFT as the distinct points on the highlighted circles. The highlighted circles correspond to gold and silver d-spacings: 4.23 nm^{-1} (2.36 Å, (111); theoretical: 2.36 Å) and 5.00 nm^{-1} (2.00 Å, (200); theoretical: 2.04 Å). Theoretical values from[4]; note, the gold and silver d-spacings are the same. Micrographs recorded on a JEM-2100 microscope (JEOL) by dropping colloid onto a holey-carbon coated Cu grid and allowing water to dry. (c) TEM image of Au@Ag nanoparticles. Core@shell structures and twinning features (resulting from the crystallisation process[5]) are visible. Figure (c) adapted with permission from *J. Phys. Chem. C*, **2017**,*121*, 1957-1963. Copyright 2017 American Chemical Society.[2]

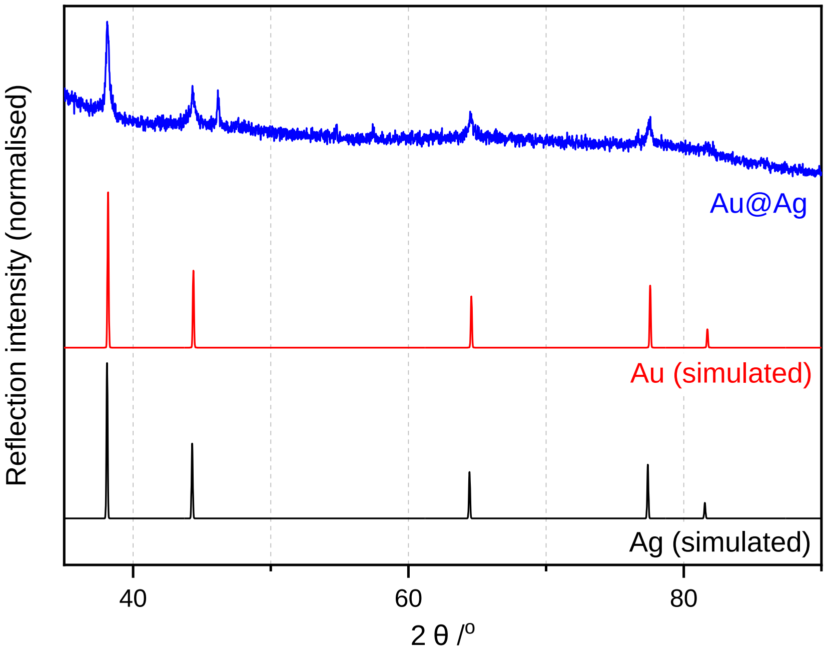

Figure S8: PXRD pattern of Au@Ag immobilised on silica, plotted alongside theoretical gold and silver FCC diffraction patterns, calculated according to ICSD 64701 and 64706[4] respectively. XRD pattern recorded on a Stadi-P diffractometer (Stoe) with a Cu Kα X-ray source.

Figure S9 compares transmission electron micrographs of the product of a colloidal nanoparticle synthesis (simultaneous gold-silver reduction; not reported in this manuscript, see reference [6] for details) in the *in-situ* cell under the X-ray beam with the product of a typical lab synthesis. This provides an understanding of the effect of the synthetic environment and conditions on the product

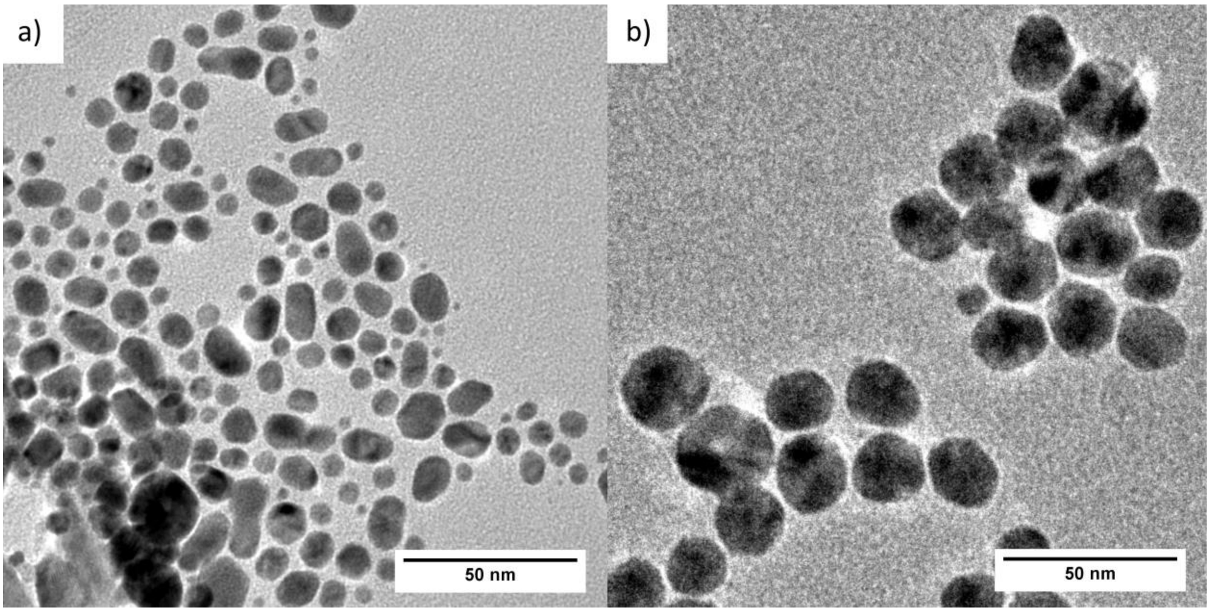

Figure S9: a) Transmission electron micrograph of colloid formed by simultaneous reduction during an *in-situ* experiment. b) Transmission electron micrograph of colloid formed by simultaneous reduction according to typical lab protocol.

Note:

This work was derived from IG's PhD thesis (available at https://discovery.ucl.ac.uk/id/eprint/10040860).

References:

1 A. Mantalidi, *Understanding the formation of gold and iron based nanomaterials using X-ray absorption spectroscopy*, PhD, University College London, 2016. https://discovery.ucl.ac.uk/id/eprint/1530968.
2 I. J. Godfrey, A. J. Dent, I. P. Parkin, S. Maenosono and G. Sankar, Structure of Gold–Silver Nanoparticles, *J. Phys. Chem. C*, 2017, **121**, 1957–1963.
3 J. Luo, W. Chu, S. Sall and C. Petit, Facile synthesis of monodispersed Au nanoparticles-coated on Stöber silica, *Colloids Surf. Physicochem. Eng. Asp.*, 2013, **425**, 83–91.
4 H. E. Swanson and E. Tatge, *Standard X-ray diffraction powder patterns. Vol. I, Data for 54 inorganic substances*, National Bureau of Standards, Washington, D.C., USA, 1953.
5 N. Uyeda, M. Nishino and E. Suito, Nucleus interaction and fine structures of colloidal gold particles, *J. Colloid Interface Sci.*, 1973, **43**, 264–276.
6 I. J. Godfrey, *Synthesis, structure and catalytic applications of monometallic and bimetallic gold-silver nanomaterials*, PhD, University College London, 2018. https://discovery.ucl.ac.uk/id/eprint/10040860